An Empirical Outdoor-to-Indoor Path Loss Model from below 6 GHz to cm-Wave Frequency Bands

Rodriguez Larrad, Ignacio; Nguyen, Huan Cong; Kovács, István Z.; Sørensen, Troels Bundgaard; Mogensen, Preben Elgaard

Published in:
I E E E Antennas and Wireless Propagation Letters

DOI (link to publication from Publisher):
10.1109/LAWP.2016.2633787

Publication date:
2017

Document Version
Accepted author manuscript, peer reviewed version

An Empirical Outdoor-to-Indoor Path Loss Model from below 6 GHz to cm-Wave Frequency Bands

Ignacio Rodriguez, Huan C. Nguyen, István Z. Kovács, Troels B. Sørensen, and Preben Mogensen

***Abstract*—This letter presents an empirical multi-frequency outdoor-to-indoor path loss model. The model is based on measurements performed on the exact same set of scenarios for different frequency bands ranging from traditional cellular allocations below 6 GHz (0.8, 2, 3.5 and 5.2 GHz), up to cm-wave frequencies (10, 18 and 28 GHz). The model has applicability similar to the typical 3GPP and ITU-R outdoor-to-indoor simplified models, including the multi-frequency formulation recently included in the 3GPP TR 38.900. This letter highlights some of the details behind these simplified models and provides additional modeling for internal multi-wall attenuation and associated shadow fading.**

***Index Terms*—Radio Propagation, Path Loss, Outdoor-to-Indoor, Penetration Loss, Indoor, Shadow Fading.**

I. Introduction

CHANNEL modeling for frequency bands above 6 GHz is gaining momentum [1]. The scarcity of available bandwidth allocations in the lower part of the radio spectrum and the need for larger continuous bandwidths in the future broadband communication systems have moved the focus of the radio propagation research activities to higher frequency bands. While most of the effort so far have been concentrated on characterizing outdoor and indoor propagation, the more complex outdoor-to-indoor propagation is still quite unexplored for these new bands [1].

As the radio signals need to penetrate into the buildings, the composition of the external facade of the different constructions plays a major role in radio propagation [2]. More in particular, old buildings (or buildings in hot climatic areas) made of light construction materials with thin walls and single-layered clear glass windows present a much lower impact on signal propagation than modern buildings (or highly-insulated buildings in cold areas). Modern and energy-efficient constructions are typically composed of thick walls made of heavily reinforced materials combined with metal-coated multi-layer windows, and can introduce up to 30-40 dB additional losses even at low frequencies [1–3]. The attenuation introduced by the external walls is typically modeled as a constant value, and there are plenty of studies reported in the literature providing such values for particular frequencies. However, there is still a need for understanding and modeling the material-dependence and frequency-dependence of the penetration loss, since the literature is rather inconclusive. The authors in [4] found a 10 dB increase in attenuation from 0.4 to 5 GHz. Differently, in [5], a constant penetration loss of 10 dB was found in the range from 0.8 to 8 GHz. Constant attenuation of 6.8 dB in the range from 0.8 to 37 GHz was recently reported in [6]. One of the first approaches to model the material and frequency dependencies was reported in [3], where a simulation based on several frequency-dependent composite models is presented for frequencies up to 60 GHz.

Once the signal gets through the external wall, it propagates inside the building along open spaces and through the inner walls. These additional indoor losses appear to be rather weakly frequency-dependent but strongly dependent on the interior characteristics of the building [1]. Similar to the penetration loss case, there is a lack of studies providing insight into the multi-frequency behavior of the indoor part of the outdoor-to-indoor radio channel. Indoor propagation loss, typically modeled as a linear attenuation factor, was reported to be 0.6 dB/m and constant with frequency in the range from 0.8 to 8 GHz in [5]. A similar finding but with slightly lower factor of 0.49 dB/m was recently reported in [6] for the extended range from 0.8 to 37 GHz. With respect to indoor wall attenuation, [3] suggests to approximate it with the low external wall attenuation given for old buildings. However, there is a lack of diversity or empirical validation in this model.

It was not until recently, in the 3GPP TR 38.900 [9], that the widely used outdoor-to-indoor path loss models proposed by the 3GPP and ITU-R standardization bodies [7, 8] were extended to frequencies above 6 GHz. This letter proposes an extension of the available statistical propagation models, including frequency-dependent formulation for internal multi-wall attenuation and the associated shadow fading, based on different sets of measurements[1] performed at 0.8, 2, 3.5, 5.2, 10, 18 and 28 GHz for the exact same set of selected scenarios. The proposed model includes frequency and material dependencies and is useful for implementation in system level simulators.

II. Measurement Campaign

The empirical data was obtained from 4 different measurement campaigns. The first one covered traditional frequency bands: 0.8, 2, 3.5 and 5.2 GHz. The second, third and fourth campaigns focused on the cm-wave spectrum with measurements at 2 and 10 GHz, 2 and 18 GHz, and 2 and 28 GHz, respectively. Since propagation at 2 GHz is well-studied in

I. Rodriguez, H. C. Nguyen, T. B. Sørensen and P. Mogensen are with the Wireless Communication Networks Section, Department of Electronic Systems, Aalborg University, Aalborg Øst 9220, Denmark (email: irl@es.aau.dk; hcn@es.aau.dk; tbs@es.aau.dk; pm@es.aau.dk).

I. Z. Kovács is with Nokia - Bell Labs, Research Center Aalborg, Aalborg Øst 9220, Denmark (email: istvan.kovacs@nokia-bell-labs.com).

P. Mogensen is also with Nokia - Bell Labs, Research Center Aalborg, Aalborg Øst 9220, Denmark (email: preben.mogensen@nokia-bell-labs.com).

[1]The authors contributed with a subset of these radio channel measurements to the model derived in [9] under the Nokia/Aalborg identifier.

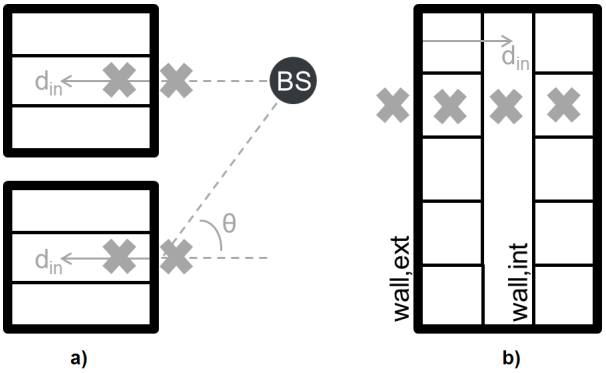

Fig. 1. Overview of the two different measurement layouts: a) shopping mall, b) office building.

the literature, it was decided to use it as common reference across the different campaigns in order to verify the correct alignment of the results and detect potential calibration errors.

All 4 campaigns were performed with a similar measurement setup. A simplified micro cell base station (BS) was emulated by using a lamppost setup with omnidirectional antennas at 7 m height (see [10] for a visual reference). Continuous wave (CW) signals at the selected carrier frequencies were simultaneously transmitted. At the receiver side, also omnidirectional antennas were mounted on a trolley at approximately 1.7 m height. The received signals at the different frequencies were simultaneously recorded by using the R&S TSMW radio network scanner. The maximum input frequency to the receiver was 6 GHz, so down-conversion was necessary for the reception of the 10, 18 and 28 GHz signals.

As depicted in Fig. 1, two different layouts were considered in the measurement campaign, where the BS was always deployed outdoors. The first one (a), aimed at exploring both penetration loss and indoor propagation. These measurements were mainly performed in shopping malls as they present long corridors that are suitable for exploring indoor propagation over long indoor distance (d_{in}) ranges. The second one (b), aimed at characterizing penetration loss. In this case, measurements were performed at different office buildings, where both external walls and internal walls were characterized.

Indoor propagation measurements were performed by moving the receiver trolley at walking speed along corridors with increasing indoor distance up to approximately 100 m. Penetration loss measurements relied on a semi-static procedure where measurements were collected at selected outdoor or indoor positions (marked with X in Fig. 1 as an example) by moving the receiver trolley back and forth over a small area in the order of a few wavelengths. These semi-static measurements were later averaged, obtaining single local mean power samples at each location.

III. Model Formulation

The proposed outdoor-to-indoor path loss model formulation is given in (1). As an extension of the 3GPP [7, 9] and ITU-R [8] models, it follows the same principles, splitting the overall outdoor-to-indoor path loss (PL) in outdoor path loss (PL_{out}), external wall attenuation ($PL_{wall,ext}$) and indoor path loss (PL_{in}).

$$PL = PL_{out} + PL_{wall,ext} + PL_{in} \quad \text{[dB]} \qquad (1)$$

At the same time, as indicated in (2), the indoor path loss is split into indoor 'open space' path loss ($PL_{in,nowalls}$) and the total internal wall loss computed as the product of the total number of penetrated internal walls (n_{walls}) by the internal average wall attenuation ($PL_{wall,int}$).

$$PL_{in} = PL_{in,nowalls} + n_{walls} \cdot PL_{wall,int} \quad \text{[dB]} \qquad (2)$$

IV. Indoor Propagation Model Extraction

In order to characterize indoor propagation, linear least square regression was applied to the measurements, obtaining linear attenuation factors (α_{in}) in dB/m. Only slopes are of interest, whereas absolute offsets are not considered as they may be different from scenario to scenario due to the different penetration losses. Based on these premises, the proposed model for indoor 'open space' path loss is given in (3). The model residuals have been included as a zero-mean Gaussian random variable (X_{SF}) with a standard deviation σ_{in} to model the random shadow fading fluctuation around the mean linear slope.

$$PL_{in,nowalls} = \alpha_{in} \cdot d_{in} + X_{SF}(0, \sigma_{in}) \quad \text{[dB]} \qquad (3)$$

Fig. 2 presents the estimated attenuation factors for the different corridors and frequencies. Each of the points was calculated as the mean regression value of all the measurements performed on that corridor for a particular frequency. As it can be seen in the figure, corridor1 presents the lowest linear attenuation. This fact can be explained with the outdoor BS location. In this case, the BS was right in front of the target corridor at normal incident angle, so a strong line-of-sight component was coupled into it. On the other hand, the other two corridors suffered from some grazing angle (θ) effect, and no direct strong line-of-sight component was present. Both situations are illustrated in the previous Fig. 1.a.

Table I collects the maximum and minimum values of the indoor linear attenuation factors per frequency. All the coefficients are very similar for all frequencies and they are aligned with the 0.49-0.6 dB/m reported in the literature for frequencies up to 8 GHz [5–8]. There is no strong frequency dependence. However, the empirical coefficients seem to slightly increase with frequency up to approximately 10 GHz, and then they are reduced again at the cm-wave frequencies, most likely due to the change to reflection-driven propagation and guiding effects at these frequencies.

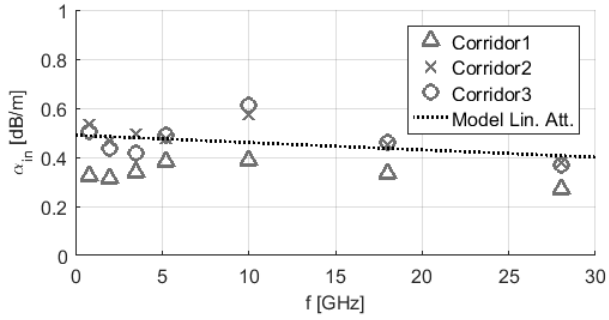

Fig. 2. Indoor linear attenuation factors (α_{in}) for the different scenarios and frequencies.

TABLE I
SUMMARY OF THE MAXIMUM AND MINIMUM INDOOR LINEAR ATTENUATION (α_{in}) AND SHADOW FADING STANDARD DEVIATIONS (σ_{in}) MEASURED FOR THE DIFFERENT FREQUENCIES

f [GHz]	0.8	2	3.5	5.2	10	18	28
$\alpha_{in,max}$ [dB/m]	0.54	0.48	0.49	0.49	0.61	0.46	0.38
$\alpha_{in,min}$ [dB/m]	0.35	0.33	0.34	0.38	0.39	0.33	0.28
σ_{in} [dB]	2.9	2.6	2.3	2.2	3.0	2.7	2.7

It should be mentioned that this kind of frequency-breakpoint was recently observed in [11] as well at around 14 GHz. With respect to the shadow fading distributions, extracted based on the separate alpha values for each frequency, they all match well to a zero-mean Gaussian distribution with very similar and low standard deviations in the order of 2.2-3 dB.

V. PENETRATION LOSS

Penetration loss is construction material-dependent, and therefore it varies with the scenarios selected for the study. The different building environments are illustrated in Fig. 3. Both external and internal wall attenuation was explored for two office buildings. The first one (a,d) is an old building composed of light construction materials and clear glass windows, which corresponds to the 'old house' configuration in [3]. The second one is a modern building ('new house' configuration in [3]) composed of thick reinforced walls and metal-coated energy-efficient windows (b,e). Both office buildings present a similar indoor layout with offices at both sides of a corridor. External wall attenuation was also investigated in a second modern building (c) composed of a metal-coated glass facade, which can be considered as another variation of the 'new house' configuration. Since it is typically of great interest for radio planning purposes for network operators, as hot-spots may be located in commercial areas, penetration loss in shopping malls and street shops (f) was also evaluated. 6 different store fronts were measured, with disparate facade compositions consisting mainly of glass (clear or metal-coated).

Penetration loss was computed as the logarithmic difference between outdoor and indoor power measurements, compensated for the outdoor propagation from the transmitter to the exterior wall, and indoor propagation from the exterior wall to the receiver. For outdoor compensation, free space propagation was assumed [1, 10] since all the outdoor measurements were performed in line-of-sight conditions. Indoor propagation was compensated by applying the average linear attenuation factors presented in Section IV for the different frequencies. As one could notice from the office building layout in Fig. 1.b, indoor measurements were done not only in the first tier of offices located closer to the external facade, but also in deeper indoor locations as the middle corridor and the second tier of offices on the other side of the corridor. In this case, by applying the previous procedure between the measurements at the different indoor depths and compensating similarly for the indoor propagation, internal wall losses could be estimated.

Fig. 3. Details of the different penetration loss scenarios explored: a) external facade, old building, b) external facade, modern building1, c) external facade modern building2, d) interior, old building, e) interior, modern building1, and f) shop.

Fig. 4 presents the estimated external wall attenuation for the selected scenarios. Several measurements at different grazing angles were done for each building at each frequency. As it can be observed, due to the light construction materials, the old building presents the lower external wall penetration loss with values lower than 15 dB, except at 28 GHz. The exception can be explained as most of the measurements at this frequency were performed at small grazing angles, which results in higher attenuation. The modern buildings present up to 15-30 dB higher attenuation than the old building across all the explored frequency range. Penetration loss in shopping areas was found as an intermediate attenuation condition between the old and modern buildings. Controlled measurements with horn antennas and normal incidence over the external facade were performed at the old and modern buildings in a previous study [2]. The resulting curves have been included as a reference in the figure and, as it can be seen, they provide a lower bound for the omnidirectional measurements presented in this letter. This provides further validation for the new set of measurements, as they were done at grazing angles and should, therefore, present higher attenuation.

Fig. 5 shows the internal wall attenuation estimated inside the old and modern office building scenarios. The measurement samples, in general over frequency, span from close to no loss up to 20 dB wall loss. As it can be noticed, there is not much difference in between the two cases. This is due to the similar interior composition, mainly made of plaster walls and wooden doors.

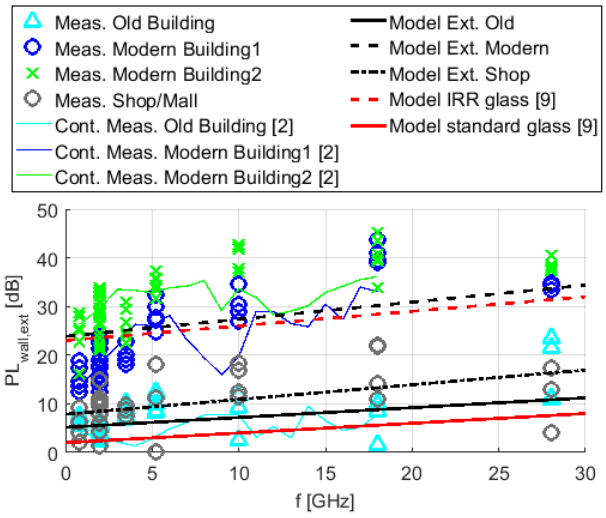

Fig. 4. External wall penetration loss for the different scenarios.

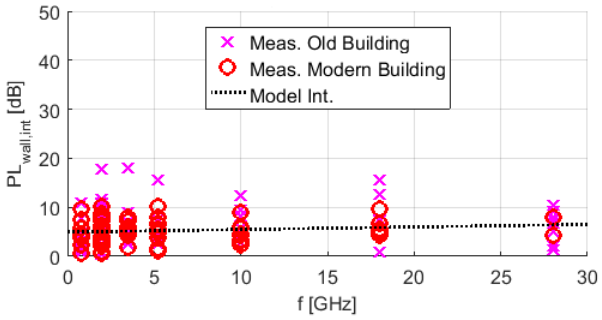

Fig. 5. Internal wall attenuation for the different scenarios.

Average external and internal wall penetration losses (μ) and standard deviations (σ) are summarized in Table II for the different frequencies and scenarios. The external wall samples from both modern buildings have been considered together as a single modern building category. Similarly, indoor wall samples from the old and modern building have been merged as a single internal wall category. Average standard deviations across the entire frequency range (σ_{wall}) are also given in the table.

TABLE II
SUMMARY OF THE AVERAGE MEASURED EXTERNAL AND INTERNAL PENETRATION LOSS (PL_{wall}) FOR THE DIFFERENT FREQUENCIES

f [GHz]	ext,old	ext,modern	ext,shop	int
	$\mu \pm \sigma$ [dB]	$\mu \pm \sigma$ [dB]	$\mu \pm \sigma$ [dB]	$\mu \pm \sigma$ [dB]
0.8	6.5±1.0	20.2±5.9	5.3±3.0	3.8±3.3
2	4.4±2.4	24.6±6.3	8.7±3.5	5.5±3.5
3.5	8.4±1.4	23.5±4.2	8.9±1.0	5.7±3.5
5.2	10.2±2.0	31.8±4.0	7.0±9.3	4.5±4.1
10	7.9±4.6	36.0±5.7	14.8±3.3	5.1±4.2
18	6.63±4.4	40.4±3.2	17.2±5.5	6.4±4.2
28	13.8±6.8	36.9±2.3	12.9±6.2	6.1±2.9
σ_{wall} [dB]	3.2	4.5	4.5	3.7

VI. Multi-frequency Formulation

Based on the empirical results, simple linear frequency-dependent models are computed for the different parameters. All the formulas, estimated from least square linear regressions, consider frequency (f) in GHz. The linear multi-frequency models have been plotted for visual reference in the corresponding Figs. 2, 4, and 5.

The multi-frequency expressions for indoor propagation (linear attenuation measured in corridors and internal wall loss) are given in (4)-(6).

$$\alpha_{in}(f) = 0.49 - 0.003 \cdot f \approx 0.49 \quad \text{[dB/m]} \tag{4}$$

$$\sigma_{in} = 2.6 \text{ dB} \tag{5}$$

$$PL_{wall,int}(f) = 4.9 + 0.05 \cdot f \ \approx 4.9 \quad \text{[dB]} \tag{6}$$

The frequency dependence observed for both the indoor linear attenuation and indoor wall loss is very weak and insignificant in consideration of the measurement accuracy, so it could be neglected. The standard deviation of the shadow fading is considered as the average value across all frequencies. The given σ_{in} value is slightly smaller than the ones provided in [9]. This is due to the fact that the measurements considered in this model are performed in indoor 'open spaces' so there is not a big impact from furnitures or other indoor structures.

With respect to external wall penetration loss, the multi-frequency models for the old building, modern building and shop scenarios are given in (7)-(9). The strongest frequency dependence is observed for the modern buildings.

$$PL_{wall,ext,old}(f) = 5.0 + 0.2 \cdot f \quad \text{[dB]} \tag{7}$$

$$PL_{wall,ext,modern}(f) = 23.9 + 0.35 \cdot f \quad \text{[dB]} \tag{8}$$

$$PL_{wall,ext,shop}(f) = 7.8 + 0.3 \cdot f \quad \text{[dB]} \tag{9}$$

The external penetration loss models for both the old and modern buildings are in good agreement with the models reported in [9] for standard multi-pane glass and IRR glass, respectively. These models have also been plotted in Fig. 4 for visual comparison.

VII. Conclusions

An extension to the existing 3GPP outdoor-to-indoor path loss models was presented in this letter. Simple linear frequency-dependent formulations were given for external wall attenuation, internal multi-wall attenuation and indoor propagation based on an extensive set of measurements performed at the exact same locations for different frequency bands ranging from 0.8 to 28 GHz. There is a clear frequency, and material, dependence for external walls, and less so for internal walls. For open indoor spaces, the model suggests frequency independent linear attenuation. The model is useful for implementation in system level simulators.

Acknowledgment

The authors would like to express their gratitude to Kim Olesen and Kristian Bank, Lab Engineers from the Department of Electronics Systems, Aalborg University, for their effort and support with the different measurement setups. The authors would also like to thank Niels T. K. Jørgensen for his participation in several phases of the measurement campaign.

References

[1] K. Haneda *et. al*, "5G 3GPP-like Channel Models for Outdoor Urban Microcellular and Macrocellular Environments", *IEEE Vehicular Technology Conference*, May 2016.
[2] I. Rodriguez *et. al*, "Radio Propagation into Modern Buildings: Attenuation Measurements in the Range from 800 MHz to 18 GHz", *IEEE Vehicular Technology Conference*, September 2014.
[3] E. Seeman *et. al*, "Outdoor-to-Indoor Coverage in High Frequency Bands", *IEEE Globecom Workshop on Mobile Communications in Higher Frequency Bands*, 2014.
[4] J. Medbo *et. al*, "Multi-Frequency Path Loss in an Outdoor to Indoor Macrocellular Scenario", *European Conference on Antennas and Propagation*, March 2009.
[5] H. Okamoto, K. Kitao and S. Ichitsubo, "Outdoor-to-Indoor Propagation Loss Prediction in 800-MHz to 8-GHz Band for an Urban Area", *IEEE Transactions on Vehicular Technology*, vol. 58, no. 3, March 2009.
[6] T. Imai *et. al*, "Outdoor-to-Indoor Path Loss Modeling for 0.8 to 37 GHz band", *European Conference on Antennas and Propagation*, April 2016.
[7] 3GPP TR 36.873 v12.0.0, Study on 3D Channel Model for LTE, June 2015.
[8] ITU-R M.2135-1, Guidelines for Evaluation of Radio Interface Technologies for IMT-Advanced, December 2009.
[9] 3GPP TR 38.900 v14.0.0, Study on Channel Model for Frequency Spectrum above 6 GHz, June 2016.
[10] I. Rodriguez *et. al*, "Path Loss Validation for Urban Micro Cell Scenarios at 3.5 GHz Compared to 1.9 GHz", *IEEE Global Communications Conference*, 2013.
[11] F. Huang *et. al*, "Propagation Characteristics of Indoor Radio Channel from 3.5 GHz to 28 GHz", *IEEE Vehicular Technology Conference*, September 2016.